IIHP: Intelligent Incident Hypertension Prediction in Obstructive Sleep Apnea

Omid Halimi Milani[1](ohalim2@uic.edu) · **Ahmet Enis Cetin**[1] (aecyy@uic.edu) · **Prasad, Bharati**[2](bpradsad@uic.edu)

[1]Department of Electrical and Computer Engineering, University of Illinois Chicago, Harrison, Chicago, IL 60607, USA
[2]Department of Medicine, University of Illinois at Chicago, Chicago, IL 60607, USA

Abstract
Obstructive sleep apnea (OSA) increases the risk of hypertension, mainly attributed to intermittent hypoxia and sleep fragmentation. Given the multifaceted pathogenesis of hypertension, accurately predicting incident hypertension in individuals with OSA has posed a considerable challenge. In this study, we leveraged Machine Learning (ML) techniques to develop a predictive model for incident hypertension up to five years after OSA diagnosis by polysomnography. We used data from the Sleep Heart Health Study (SHHS), which included 4,797 participants diagnosed with OSA. After excluding those with pre-existing hypertension and Apnea Hypopnea Index (AHI) values below 21 per hour, we had 671 participants with five-year follow-up data. We adopted two distinct methodologies. We first implemented adaptive convolution layers to extract features from the signals and combined them into a 2D array. The 2D array was further processed by a 2D pre-trained neural network to take advantage of transfer learning. Subsequently, we delved into feature extraction from full-length signals across various temporal frames, resulting in a 2D feature array. We studied the use of various 2D networks such as MobileNet, EfficientNet, and a family of RESNETs. The best algorithm achieved an average area under the curve of 72%. These results suggest a promising approach for predicting the risk of incident hypertension in individuals with OSA, providing tools for practice and public health initiatives.

Keywords Machine Learning (ML) · Obstructive Sleep Apnea (OSA) · Sleep Heart Health Study (SHHS) · Incident Hypertension

1 Introduction

Obstructive sleep apnea (OSA) is a condition characterized by intermittent hypoxia and sleep fragmentation, which propagates hypertension via mechanisms such as sympathetic activation and inflammation. OSA also raises the likelihood of developing hypertension during nighttime. [1-4]. Notably, specific patterns of apnea, such as Rapid Eye Movement (REM) sleep-related OSA, could contribute to OSA-associated hypertension [5]. Additional sleep-related factors, like reduced slow-wave sleep (SWS) and short sleep duration, are associated with hypertension, independent of OSA [6, 7]. Ren and colleagues conducted a study examining the association, between sleep duration, obstructive sleep apnea (OSA) and hypertension in a group of 7,107 OSA patients and 1,118 primary snorers. The findings from polysomnography indicated that individuals who slept for 5 to 6 hours had a 45% risk of developing hypertension while those who slept, than 5 hours had an 80% increased risk. These results were independent of any factors that could potentially influence the outcome. [8].

Around 30% of people, in the United States are affected by hypertension, which can lead to dysfunction in organs. Treating obstructive sleep apnea (OSA) has been shown to lower the risk of developing hypertension. [9]. However, accurately predicting the onset of hypertension in individuals with OSA remained a challenge due to the complex pathogenesis of hypertension.

This study leveraged deep Machine Learning (ML) techniques to develop a predictive model for incident hypertension up to five years after OSA diagnosis by polysomnography. The novel ML-based method utilized polysomnography signal conversion and a composite deep CNN model to transform the polysomnography signals into image datasets to predict incident hypertension. During the training process, additional static information for each patient was incorporated, including age, sex, race, body mass index, baseline systolic, and diastolic blood pressure. Our study aimed to accelerate precision

medicine in managing hypertension and preventive healthcare by integrating polysomnography and clinical data analytics. This research could equip healthcare professionals with tools to address the significant health burden posed by OSA and hypertension [10].

We hypothesized that a comprehensive approach involving the simultaneous input of time-series physiological signals measuring sleep (EEG), ventilatory impairment and hypoxia, and cardiac autonomic dysregulation (electrocardiogram and photoplethysmography-derived heart rate variability and pulse transit time) preserved the temporal correlations between multiple physiological perturbations in OSA and could provide a robust prediction of incident hypertension in OSA. These signals were included in polysomnography, a widely available diagnostic test for OSA. Thus, we extracted multiple features from the polysomnography signals in the SHHS participants with moderate to severe OSA. [11, 12]. Before feature extraction, rigorous preprocessing steps were employed, involving removing artifacts and applying a bandpass filter to eliminate any remaining noise. Next, we explored whether the addition of clinical factors that independently affected the risk of hypertension (age, sex, race, body mass index, and baseline systolic and diastolic blood pressure) improved the prediction performance of the ML model.

The paper advocates using timing interval windowing as an effective approach to feature extraction. This technique enabled the creation of a structured 2D array, facilitating the application of transfer learning. Additionally, a model fine tuning process was applied to enhance its adaptability to the specific characteristics of the sleep data. The paper introduces a novel adaptive feature extractor, designed from the ground up. This extractor was meticulously crafted to adapt to the intricacies of the sleep data, ensuring a comprehensive and accurate representation of the underlying patterns. We analyzed the signal using networks. Initially, we abstracted details from the study, constructed an image based on these details, and customized the initial EfficientNet model, which was pretrained, for the task by adjusting its layers. To overcome limitations posed by the number of features and limited memory capacity, a 32-bit model was utilized. Our second approach focused on using networks (CNNs) to extract features from the signals. We created a 2D array that represented segments of the signals and their associated features. These features included counts of arousal and respiratory events, as well as statistical measures like mean, standard deviation, skewness, and kurtosis for heart rate variability analysis. After exploring timing intervals, we determined that a window length of 10 minutes showed promising results.

The proposed methodology underwent a rigorous evaluation through a 10-fold cross-validation approach to examine the model's generalizability. The results were subsequently summarized, comparing models and methods to cutting-edge approaches.

2 Related works

In recent years, there has been a growing recognition of the limitations associated with conventional manual sleep stage scoring, which simplifies the analysis of electroencephalogram (EEG) temporospectral and frequency domains. This scoring method is inherently subjective and can lead to variations between different scorers due to the application of visual-based rules [13]. To reduce this variability, researchers used power spectral density (PSD) analysis of EEG signals, which objectively examines sleep EEG microarchitecture. This approach enables the decomposition of EEG brain waves across various power frequency bands, ranging from slow wave activity (delta EEG power, 1–4 Hz) to fast-frequency activity (beta EEG power, 18–30 Hz), achieved through implementing fast Fourier transform algorithms. At a microarchitecture level, slow wave sleep (SWS) is characterized by high delta power, indicative of deep sleep. Numerous studies have suggested that quantitative EEG analysis may yield more sensitive biomarkers for adverse health outcomes in OSA compared to traditional sleep scoring methods [14-17]. However, there is a paucity of research investigating the relationship between sleep microarchitecture and the future development of hypertension in OSA. Berger et al. recently reported that low delta power in non-REM sleep is independently associated with the risk of developing hypertension, confirming the previously noted relationship of SWS with incident hypertension [18]. Another study relied on complex feature engineering to examine 27 unselected clinical predictors, encompassing demographic characteristics, lifestyle behaviors, and OSA severity (apnea-hypopnea index; AHI, and oximetry indices) [19].

Ruitong et al. adopted a pulmonary physiology-based approach to predicting the onset of hypertension by including pulmonary function measurements and polysomnography-derived indices using a penalized regression and Elastic Net model [20]. A recent study introduced cSP (sleep and pulmonary) phenotypes, which combines spirometry and overnight polysomnography measures to predict hypertension occurrence in the Sleep Heart Health Study (SHHS). The researchers employed penalized regression to select features and estimate effect size simultaneously[14]. The SHHS dataset encompasses

a variety of physiological signals, including sleep EEG and electrooculogram (EOG), electrocardiogram (ECG), electromyogram (EMG), ventilatory effort, nasal airflow, photoplethysmography-derived oximetry, snoring, and body position. Employing rigorous signal processing techniques, such as filtering, segmentation, and feature extraction, our analysis aimed to unravel the intricate patterns embedded within these signals [11, 12].

In the following sections, we explain our methodology, present our findings, and discuss the implications of our research within the context of practice and public health initiatives. Section 3 detailed our methodology, covering feature extraction, machine learning models, and innovative techniques. Section 4 briefly summarizes results, comparing methods with references. The conclusion section discusses the implications of this study and future research.

3 Methods

In this study, we explored two methodologies for predicting incident hypertension in individuals with moderate to severe OSA. One notable enhancement to our approach involved the integration of a convolution layer designed to automatically extract features from each signal. This layer dynamically adjusted itself during training, facilitating the automatic extraction of features and identification of crucial patterns within the data. However, it came with a computational expense, leading us to modify the computation to 32-bit, albeit extending the training time to 10 days. In an alternative approach, we devised a system to extract features directly from the signals. The extracted features from the entire signals were then converted into a 2D array. Each row in the array represented the feature representation of a signal, enabling the capture of temporal information from diverse signals through the application of convolution kernels. This method was not only easy to train but also faster, allowing our server to complete the training process within 4 hours. Overall, our findings indicated that the second method, with its efficiency and superior model performance, stood out among the experiments. Nevertheless, with the utilization of faster and more capable servers, coupled with an expanded dataset, there is potential for reconsidering and refining the other two methods. The implementation details are listed in the following sections. Then, we highlighted the details of the findings and reported the performance comparison with the state-of-the-art methods.

Prior to conducting any data analysis, we implemented a preprocessing step for each signal. Specifically, a portion of the SaO2 Signal, along with OX, underwent processing in Module 1. Notably, the presence of numerous sparks due to power outages necessitated their removal using the Spark Remover filter. To address this issue, we employed Module 1 and Filter 1 as depicted in Figure 1.

Module 1 Modifier
Inputs: SaO2 Signal and OX Signal
Output: Verified Signal SaO2_OX
1: Insert the signals
2: Align the signals in time domain
3: Omit/keep SaO2 samples in which the OX is 2/1 or 0.

(a) Reconstructing the SaO2 signal based on OX signal in shhs Dataset.

Filter 1 Spark remover
Inputs: Verified Signal SaO2_OX
Output: Modified SaO2_OX
1: Insert the SaO2_OX
2: Detect sudden drop in the signal and remove the sparks
3: Interpolate to fill out the removed sparks in Verified Signal SaO2_OX

(b) The filter for removing the power outage

Fig. 1 As indicated in the dataset, we can utilize OX for signal validation in each second, and it is essential to remove sparks, as described in Module 1 and Filter 1 respectively

3.1 Intelligent Signal-Based Method for Predicting Incident Hypertension from Obstructive Sleep Apnea

The intelligent signal-based method involved extracting features from signals using convolutional layers to construct an image from the derived features. These features were then inputted into the pre-trained EfficientNet, with fine-tuning applied to the first convolutional layers and the final classifier layer. The overall methodology was depicted in Figure 2, where the red boxes represented the kernels, scaled according to the sampling frequencies of the signals. Following the application of convolution to each signal, the results from different signals were consolidated and passed through a converter, constituting

another convolutional layer that standardized the input for the EfficientNet. Consequently, the 11 channels were condensed to 3 channels before being fed into the EfficientNet. All CNN models were trained, in addition to the EfficientNet classifier. The structure of the EfficientNet aligned with the specifications outlined in Table 1.

The signals' names in this study were based on the SHHS study. The SHHS signal comprised vital parameters for sleep analysis. "sao2_OX" monitored blood oxygen levels, EEG tracked brain activity, and EMG recorded muscle activity. EEG (sec) provided additional brain activity details. EOG(L) and EOG(R) monitored eye movements. THOR and ABDO measured respiratory effort, POSITION recorded body posture, and NEW AIR tracked fresh air introduction. This diverse set of signals allowed for a detailed assessment of sleep patterns, respiratory functions, and positional variables, contributing to a comprehensive understanding of sleep health [11, 12].

Table 1 The structure of the EfficientNet.

Layer	Output Size	Details
Input Layer	$3 \times 78 \times 54$	Input Image with 78×54 pixels
Convolutional Layers	$32 \times 96 \times 96$	Standard Conv 3×3, Stride 2
Depthwise Separable	$32 \times 96 \times 96$	Depthwise Conv 3×3, Pointwise Conv 1×1
Depthwise Separable	$16 \times 96 \times 96$	Depthwise Conv 3×3, Pointwise Conv 1×1
Depthwise Separable	$24 \times 48 \times 48$	Depthwise Conv 3×3, Pointwise Conv 1×1
Inverted Residual	$40 \times 48 \times 48$	
Inverted Residual	$80 \times 24 \times 24$	
Depthwise Separable	$80 \times 24 \times 24$	Depthwise Conv 3×3, Pointwise Conv 1×1
Depthwise Separable	$112 \times 12 \times 12$	Depthwise Conv 3×3, Pointwise Conv 1×1
Inverted Residual	$192 \times 12 \times 12$	
Depthwise Separable	$192 \times 12 \times 12$	Depthwise Conv 3×3, Pointwise Conv 1×1
Depthwise Separable	$320 \times 6 \times 6$	Depthwise Conv 3×3, Pointwise Conv 1×1
Max Pooling	$320 \times 6 \times 6$	Max Pooling 3×3, Stride 2
Fully Connected	1280	
Fully Connected	1	Final output with softmax activation

Figure 2 depicted the structure of the methodology and how the data fed into our model after different artifacts from the signals were removed. This approach faced computational challenges when applied to a single patient's data, given the extended signal duration (around 9 hours) with approximately 4 million data points in the ECG signal alone. The combination of signals resulted in a high feature count, exacerbated by a limited dataset unsuitable for full model training. To overcome these constraints, a proposed solution involved a novel approach to feature extraction through windowing.

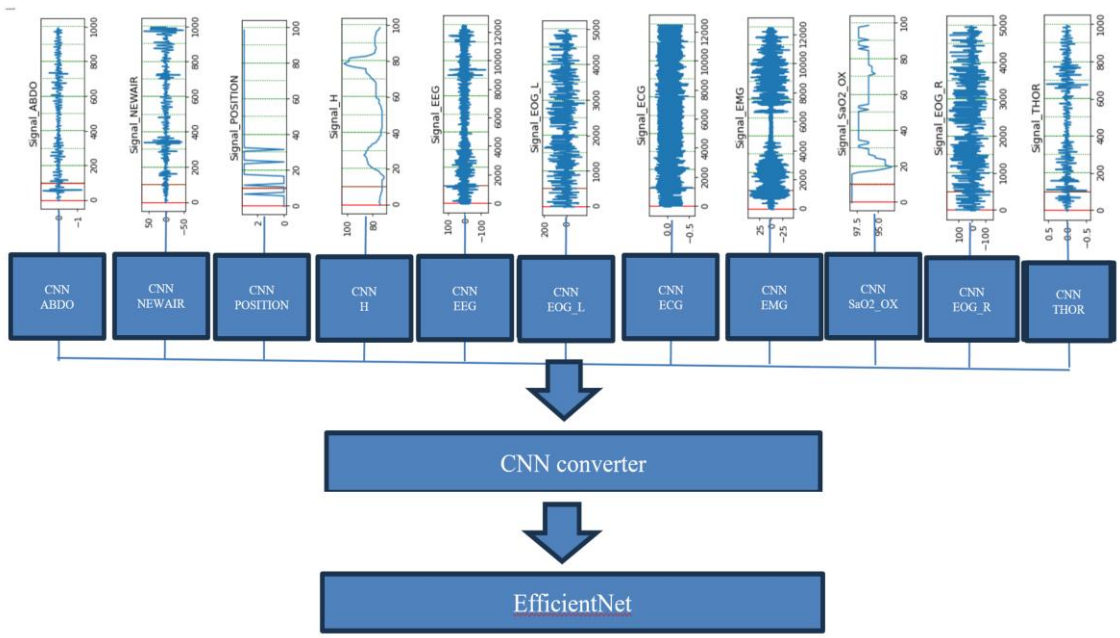

Fig. 2 Feature extraction from signal windows using Convolutional Neural Networks (CNN). The CNN architecture enhances pattern recognition and understanding.

3.2 Intelligent Feature-Based Method for Predicting Incident Hypertension from Obstructive Sleep Apnea

The occurrence of hypertension appears to be non-trivial to pinpoint within the signals. Therefore, we adopted a holistic approach, considering the entire signal rather than an event-based strategies. In this method, we applied various windowing sizes to the signals and extracted the relevant features from each segment using different CNNs processing individual signals. These features were then organized into a 2D array, where each column represented a segment of the signal along with its corresponding features. The features encompassed the frequency of arousal events, respiratory events, heart rate variability, as well as statistical measures like minimum, standard deviation, mean, skewness, kurtosis, maximum, and median derived from 11 distinct signals.

Several statistical features extracted from the Signals. The mean of a dataset in equation 1, denoting the average value, was calculated using the following formula where $\bar{x}$ was the mean, n was the number of data points, and x_i are the individual data points.

$$\bar{x} = \frac{1}{n}\sum_{i=1}^{n} x_i \tag{1}$$

The standard deviation, as shown in Equation 2, measured the spread or dispersion of the data points around the mean. [21]. It was calculated as:

$$\sigma = \sqrt{\frac{1}{n}\sum_{i=1}^{n}(x_i - \bar{x})^2} \tag{2}$$

The symbol σ represents the deviation n stands for the number of data points x̄ represents the mean. Xi refers to each individual data point. Skewness is a measure of how asymmetrical the probability distribution of a valued variable is. A positive skewness, calculated using equation 3 as mentioned in [22] suggests a tail, on the side whereas a negative skewness indicates a longer tail, on the left side.

$$\text{Skewness} = \frac{\sum_{i=1}^{n}(x_i - \bar{x})^3}{n\sigma^3} \tag{3}$$

Kurtosis, as calculated in the equation, measured the "tailedness" of the probability distribution. It described the shape of the distribution's tails in relation to the normal distribution. [22].

$$\text{Kurtosis} = \frac{\sum_{i=1}^{n}(x_i - \bar{x})^4}{n\sigma^4} - 3 \tag{4}$$

Another crucial feature involved heart rate variability (HRV), a parameter integral to the assessment of cardiac health and autonomic nervous system function. HRV was determined by detecting peaks and variations in the time intervals between successive heartbeats and corresponding HRV features calculated as showed in Figure 3. This metric provided valuable insights into the adaptability and resilience of the cardiovascular system, reflecting the dynamic interplay between the sympathetic and parasympathetic branches of the autonomic nervous system [23, 24].

Feature	Calculation
Mean RR Interval	$\text{Mean}(RR)$
Standard Deviation of RR Intervals (SDNN)	$\text{SDNN}(RR)$
RMSSD	$\sqrt{\text{Mean}((RR_{i+1} - RR_i)^2)}$
pNN50	Percentage of successive RR intervals differing by more than 50 ms
Minimum Heart Rate (HR)	$60000/\text{Max}(RR)$
Maximum HR	$60000/\text{Min}(RR)$
Mean HR	$60000/\text{Mean}(RR)$
HR Standard Deviation	Standard deviation of HR
NN50	Number of pairs of successive RR intervals differing by more than 50 ms
pNN50	Percentage of successive RR intervals differing by more than 50 ms

Fig. 3 The Heart Rate Variability (HRV) Calculation Algorithm is a systematic process designed to extract essential features from raw Electrocardiogram (ECG) signals.

Figure 4 outlined the steps involved in constructing the given dataset. Depending on the window timing, different features were extracted from the signals. These included minimum, standard deviation, average, skewness, kurtosis, maximum, and median within the T-minute interval of the signal. Additionally, the count of respiratory and arousal events within that T-minute interval was recorded. Furthermore, heart rate variability was derived from the ECG signals. Together, these components constituted the first column in the 2D array. Subsequent columns followed the same pattern, with the window shifting to the right with a stride of T minutes.

The potential of employing Finite Impulse Response (FIR) and Infinite Impulse Response (IIR) filters for data augmentation was also explored. These filters were applied to the signal prior to extracting features from them. Different

orders of 4, 6, and 8 were applied to the signals for FIR filters, and the impulse response of an FIR filter was a sequence of finite duration. Different orders of 18, 20, and 22 were applied to the signals for IIR filters [25].

The Convolutional Neural Network (CNN) was a widely adopted and highly efficient trainable model for tasks related to image classification. Its effectiveness in categorizing images into specific classes had made it an indispensable tool in various computer vision applications. By utilizing 2-D convolution operations, CNNs were able to extract meaningful information from images. These convolution layers acted as feature extractors, capturing crucial patterns, textures, and structures present in the input images.

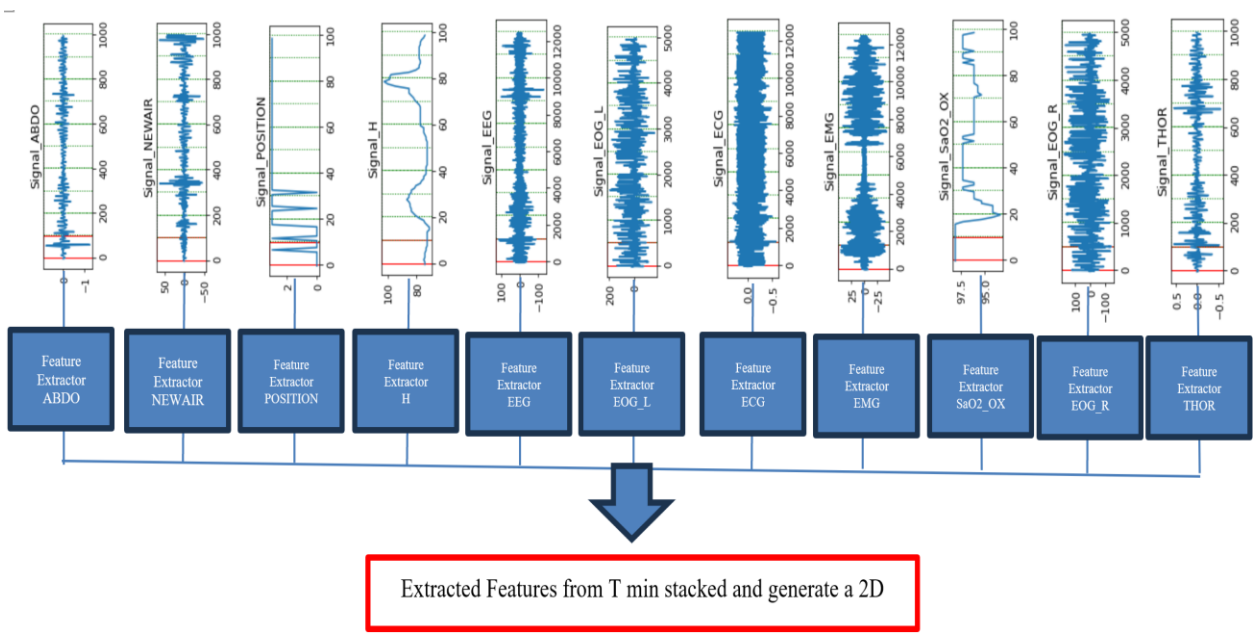

Fig. 4 Feature extraction from signal windows using various statistical metrics involved computing features such as maximum, minimum, average, standard deviation, kurtosis, skewness, heart rate variability, number of arousal events, and number of respiratory events. These diverse features contributed to comprehensive pattern recognition and understanding within the signal processing framework.

In recent years, significant progress has been made in the field of computer vision, leading to the development of numerous CNN architectures, each aiming to achieve higher accuracy on large benchmark datasets. Among these architectures, ResNet stands out for effectively addressing the vanishing gradient problem in deep CNNs. Through the introduction of residual connections, information flows directly through the network, allowing ResNet to achieve greater depth, expressiveness, and improved image classification performance.

Another notable advancement in CNN architectures was MobileNet. These models were characterized by their lightweight and resource-efficient nature, making them well-suited for deployment on less powerful devices such as mobile phones and embedded systems. They utilized depthwise separable convolutions, which significantly reduced parameters and computations compared to traditional convolutions. This resulted in faster inference times and optimal performance for real-time applications on resource-constrained devices. [26]. Like MobileNet, ShuffleNet is a special kind of computer program for mobile phones. It helps them do things quickly without using too much power. ShuffleNet has two clever parts that work together to save power and still do things accurately [27].

EfficientNet was a revolutionary CNN architecture that merged the advantages of ResNet and MobileNet, addressing their limitations. It employed compound scaling to optimize network depth, width, and resolution simultaneously with a single scaling coefficient. This enabled a balanced trade-off between model size and accuracy, enhancing versatility and efficiency for diverse image classification tasks. The architecture integrated depthwise separable convolutions from

MobileNet and residual connections from ResNet, achieving state-of-the-art performance on benchmark datasets with improved computational efficiency [28].

In this study, we primarily employed EfficientNet-B0 as our base model, comparing its results with various other CNN architectures. The general architecture of EfficientNet-B0 is detailed in Table 1. Our proposed algorithm built upon EfficientNet as the baseline, incorporating comparisons with other models. The input image shape consisted of a 2D array where rows represented features, and columns denoted the specified window time, set at 10 minutes for Table 1. This 2D array was replicated and input as different channels to EfficientNet, with all CNN model classifiers being fine-tuned.

The static data was also experimented with in different models. The way the static data was included in the decision-making process varied, as described in Figure 5. One approach involved adding the static data to the final layer of the pretrained models and fine-tuning all the weights together to satisfy the desired output. Another approach involved adding another fully connected layer and concatenating the static data in the second layer, followed by fine-tuning all the weights together. In an effort to improve our abilities, we decided to combine two models: one based on EfficientNetB0 and the other using the ConvexNet architecture. However, the combination of these models did not noticeably enhance our performance. This suggests that both models may have generated predictions resulting in synergy [29, 30].

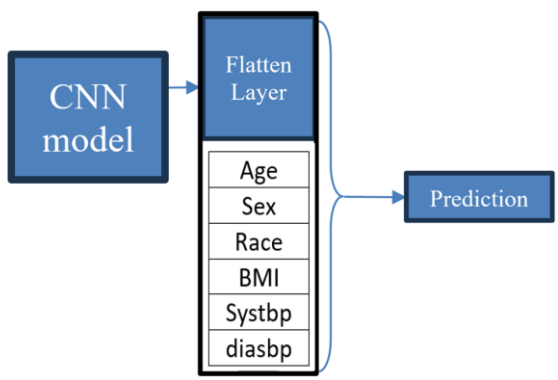

a) Static data was added along with the flattened output of the model.

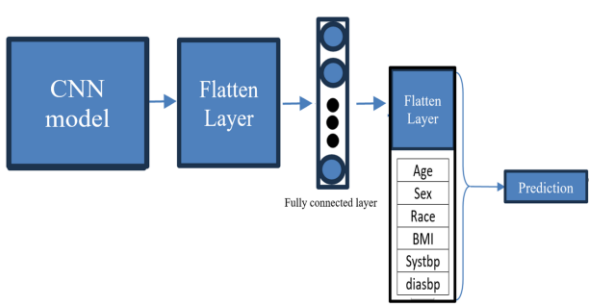

b) One more fully connected layer was added, and then static data was incorporated along with the flattened output of the model.

Fig. 5. The static data, including BMI (body mass index), Sysbp (systolic blood pressure), and Diasbp (diastolic blood pressure), was added to the model. a) static_v1, b) static__v2

4 Results

We employed various metrics to evaluate the robustness of our approaches. To assess the model's performance, we utilized 10-Fold cross-validation to mitigate potential biases. The process for implementing 10-fold cross-validation was outlined in Figure 6. This involved partitioning the training data into training and validation sets, with each round validating the data against the trained model. Ultimately, the results were averaged across the 10 different folds.

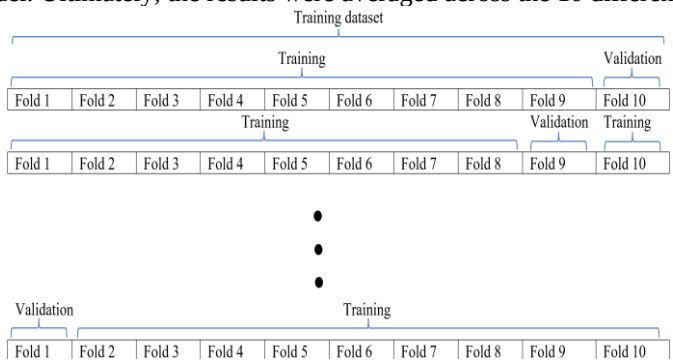

Fig. 6. 10-fold cross validation method

We used equations 7, 8 and 9 to calculate the accuracy, area, under the curve (AUC) using rate (TPR) and false positive rate (FPR) respectively. The AUC was determined by plotting TPR, against FPR at classification thresholds. It helped us measure how well the model can distinguish between classes with values indicating performance.

$$\text{Accuracy} = \frac{\text{Number of Correct Predictions}}{\text{Total Number of Predictions}} \tag{7}$$

$$\text{TPR} = \frac{\text{True Positives}}{\text{True Positives} + \text{False Negatives}} \tag{8}$$

$$\text{FPR} = \frac{\text{False Positives}}{\text{False Positives} + \text{True Negatives}} \tag{9}$$

Choosing the optimal range for sensitivity and specificity, or their equivalents TPR and FPR, was crucial for our study. Sensitivity (True Positive Rate) took precedence when detecting positive cases was critical, while specificity (1 - False Positive Rate) was vital for minimizing false alarms.

In Approach 1 and 2, we utilized Convolutional Neural Networks (CNNs). We explored state-of-the-art pretrained models for transfer learning after preprocessing the data points. The input data fed into the model consisted of 2D arrays, obtained by applying varying windowing techniques on the signal proportional to the sampling frequencies. The difference between approach 1 and 2 was about their feature extraction methods. We conducted experiments with different window lengths and assessed the model's performance under various intervals to identify the near-optimal windowing strategy. Our findings indicated that a 10-minute window length yielded the most favorable results compared to other timing intervals with the second approach. Additionally, we investigated both Adam and SGD as optimizers, coupled with schedular techniques, to explore the solution space more effectively.

Table 2 The structure of different transfer learning models were examined through various experiments. Experiments were conducted on the images (2D arrays) generated from the extracted features: a) 2D arrays derived from the extracted features with 10-minute intervals and the Adam optimizer. b) 2D arrays derived from the extracted features with 10-minute intervals and the SGD optimizer.

Models/Results	Accuracy	AUC	Sensitivity	Specificity
mobilenet_v2	66	63	63	71
mobilenet_v3	64	60	70	62
EfficientNetB0	**69**	**72**	75	68
EfficientNetB0_Static_v1	68	69	76	64
EfficientNetB0_Static_v2	66	66	74	63
Resnet10	63	60	64	62
Resnet18	61	57	59	65
Convexnet	68	65	58	77
ConvexnetS	66	66	68	69
Mobilenet_v2_Static_v1	64	63	68	62
Mobilenet_v2_Static_v2	64	62	67	67
Ensemble_efficinet_convex	64	60	59	68

a) The experiment involved 10-minute time intervals with the Adam optimizer.

Models/Results	Accuracy	AUC	Sensitivity	Specificity
mobilenet_v2	65	63	61	72
mobilenet_v3S	62	58	64	63
EfficientNetB0	**69**	**68**	69	71
EfficientNetB0_Static_v1	68	68	75	67
EfficientNetB0_Static_v2	67	65	71	66
Resnet10	61	57	61	61
Resnet18	61	56	56	67
Convexnet	67	66	64	72
ConvexnetS	66	66	67	69
Mobilenet_v2_Static_v1	65	63	67	65
Mobilenet_v2_Static_v2	64	62	65	64
Ensemble_efficinet_convex	63	60	60	67

b) The experiment involved 10-minute time intervals with the SGD optimizer.

Table 3 a) 2D array derived from the extracted features with 60-minute intervals and Adam optimizer. b) 2D array derived from the extracted features with 60-minute intervals and SGD optimizer

Models/Results	Accuracy	AUC	Sensitivity	Specificity
mobilenet_v2	65	61	59	72
mobilenet_v3S	64	62	67	65
EfficientNetB0	**68**	**68**	70	70
EfficientNetB0_Static_v1	68	68	71	69
EfficientNetB0_Static_v2	67	66	69	67
Resnet10	62	59	60	64
Resnet18	60	54	58	63
Mobilenet_v2_Static_v1	64	62	66	64
Mobilenet_v2_Static_v2	64	62	66	63

a) The experiment involved 60-minute time intervals with the Adam optimizer.

Models/Results	Accuracy	AUC	Sensitivity	Specificity
mobilenet_v2	65	62	60	72
mobilenet_v3S	64	61	67	64
EfficientNetB0	69	68	69	71
EfficientNetB0_Static_v1	68	68	71	69
EfficientNetB0_Static_v2	67	66	69	67
Resnet10	62	59	60	64
Resnet18	60	54	57	64
Mobilenet_v2_Static_v1	64	61	65	64
Mobilenet_v2_Static_v2	63	61	66	62

b) The experiment involved 60-minute time intervals with the SGD optimizer.

In addition to the 10-minute and 60-minute intervals, we investigated various timing intervals. The results for the best models at different timing intervals were summarized in Table 4.

Table 4 The results for different windowing on the signal for feature extraction.

Models/Results	Best Accuracy	AUC	Sensitivity	Specificity
9 minutes				
Efficientnet_b0	67	67	74	64
Convexnet	67	66	63	72
10 minutes				
EfficientNetB0	69	72	75	68
Convexnet	68	65	58	77
11 minutes				
Efficientnet_b0	66	65	69	67
Convexnet	67	66	66	71
12 minutes				
Efficientnet_b0	66	64	69	67
Convexnet	67	64	66	69
13 minutes				
Efficientnet_b0	67	65	69	68
Convexnet	66	63	66	67
14 minutes				
Efficientnet_b0	67	66	69	69
Convexnet	66	63	66	68
15 minutes				
Efficientnet_b0	67	66	69	68
Convexnet	66	63	66	68

The overall results for different models and methods, along with a comparison to the state of the art, were presented in Table 5.

Table 5 The results for different windowing on the signal for feature extraction were examined.

Models/Results	Best Accuracy	AUC	Sensitivity	Specificity
mobilenet_v2	66	63	63	71
mobilenet_v3	64	60	70	62
EfficientNetB0	**69**	**72**	75	68
EfficientNetB0_Static_v1	68	68	71	69
EfficientNetB0_Static_v2	67	66	69	67
Resnet10	63	60	64	62
Resnet18	61	57	59	65
Convexnet	68	65	58	77
Convexnet_Static_v1	66	66	68	69
Mobilenet_v2_Static_v1	64	63	68	62
Mobilenet_v2_Static_v2	64	62	67	67
Ensemble_efficinet_convex	64	60	59	68
EfficinetNetb0_FIR_IIR	64	60	59	68
cSPPSG [11]	-	71	-	-
AHI [11]	-	67	-	-
EfficinetNetb0_CNN_feature	65	63	68	63

EfficientNetB0 emerged as the top-performing model with the highest Best Accuracy (69%) and AUC (72%), showcasing its effectiveness. Other models, such as Convexnet also demonstrated competitive performance across different metrics. The table served as a comprehensive overview of the comparative performance of various models in the given study context.

5 Conclusion

In this research, we investigated methods of extracting features from polysomnography, using the SHHS dataset. Before extracting the features, we prepared the data by removing any distortions and applying a filter to eliminate remaining noise. Additionally, we used timing interval windowing as a method for feature extraction. This allowed us to create a 2D array that made it easier to apply transfer learning techniques. We fine-tuned our model, making it more adaptable to the characteristics of sleep data. Furthermore, we introduced a feature extractor that was specifically designed for this study. This extractor was created with attention to detail to adapt well and accurately represent patterns in polysomnography data. We evaluated our proposed methodology using a ten-fold cross-validation technique to assess the potential generalizability of the model. Our contributions, such as developing feature extraction methods and implementing a tuned adaptive feature extractor, significantly improved the accuracy of predicting incident hypertension in individuals with OSA. When combined with AI and Machine Learning techniques, these new developments in methodology may provide clinicians with tools for early diagnosis and treatment of hypertension in OSA populations. We had a memory limitation due to the high number of features for each patient and the relatively small number of patients in the dataset. Our future research will concentrate on integrating diverse data modalities and exploring innovative feature extraction techniques. Ethical

considerations and validation of the novel models in larger longitudinal studies in diverse populations will advance personalized approaches to managing hypertension for individuals with OSA.

References

1. Peppard, P.E., et al., *Prospective study of the association between sleep-disordered breathing and hypertension.* New England Journal of Medicine, 2000. **342**(19): p. 1378-1384.
2. Dudenbostel, T. and D. Calhoun, *Resistant hypertension, obstructive sleep apnoea and aldosterone.* Journal of

human hypertension, 2012. **26**(5): p. 281-287.
3. Genta-Pereira, D.C., et al., *Nondipping blood pressure patterns predict obstructive sleep apnea in patients undergoing ambulatory blood pressure monitoring.* Hypertension, 2018. **72**(4): p. 979-985.
4. O'Connor, G.T., et al., *Prospective study of sleep-disordered breathing and hypertension: the Sleep Heart Health Study.* American journal of respiratory and critical care medicine, 2009. **179**(12): p. 1159-1164.
5. Mokhlesi, B., et al., *Obstructive sleep apnea during REM sleep and hypertension. results of the Wisconsin Sleep Cohort.* American journal of respiratory and critical care medicine, 2014. **190**(10): p. 1158-1167.
6. Javaheri, S., et al., *Slow-wave sleep is associated with incident hypertension: the sleep heart health study.* Sleep, 2018. **41**(1): p. zsx179.
7. Wang, L., et al., *The association between sleep duration and hypertension: a meta and study sequential analysis.* Journal of Human Hypertension, 2021. **35**(7): p. 621-626.
8. Ren, R., et al., *Objective but not subjective short sleep duration is associated with hypertension in obstructive sleep apnea.* Hypertension, 2018. **72**(3): p. 610-617.
9. Marin, J.M., et al., *Association between treated and untreated obstructive sleep apnea and risk of hypertension.* Jama, 2012. **307**(20): p. 2169-2176.
10. Casey Jr, D.E., et al., *2019 AHA/ACC clinical performance and quality measures for adults with high blood pressure: a report of the American College of Cardiology/American Heart Association Task Force on Performance Measures.* Circulation: Cardiovascular Quality and Outcomes, 2019. **12**(11): p. e000057.
11. Quan, S.F., et al., *The sleep heart health study: design, rationale, and methods.* Sleep, 1997. **20**(12): p. 1077-1085.
12. Zhang, G.-Q., et al., *The National Sleep Research Resource: towards a sleep data commons.* Journal of the American Medical Informatics Association, 2018. **25**(10): p. 1351-1358.
13. Schulz, H., *Rethinking sleep analysis: Comment on the AASM manual for the scoring of sleep and associated events.* Journal of Clinical Sleep Medicine, 2008. **4**(2): p. 99-103.
14. Appleton, S.L., et al., *Quantitative electroencephalography measures in rapid eye movement and nonrapid eye movement sleep are associated with apnea–hypopnea index and nocturnal hypoxemia in men.* Sleep, 2019. **42**(7): p. zsz092.
15. D'Rozario, A.L., et al., *Quantitative electroencephalogram measures in adult obstructive sleep apnea–potential biomarkers of neurobehavioural functioning.* Sleep medicine reviews, 2017. **36**: p. 29-42.
16. Lechat, B., et al., *A novel electroencephalogram-derived measure of disrupted delta wave activity during sleep predicts all-cause mortality risk.* Annals of the American Thoracic Society, 2022. **19**(4): p. 649-658.
17. Parker, J.L., et al., *The association between obstructive sleep apnea and sleep spindles in middle-aged and older men: a community-based cohort study.* Sleep, 2022. **45**(3): p. zsab282.
18. Berger, M., et al., *Association Between Sleep Microstructure and Incident Hypertension in a Population‐Based Sample: The HypnoLaus Study.* Journal of the American Heart Association, 2022. **11**(14): p. e025828.
19. Shi, Y., et al., *Prediction model of obstructive sleep apnea–related hypertension: Machine learning–based development and interpretation study.* Frontiers in Cardiovascular Medicine, 2022. **9**: p. 1042996.
20. Li, R., et al., *A composite sleep and pulmonary phenotype predicting hypertension.* EBioMedicine, 2021. **68**.
21. Muntner, P., et al., *Potential US population impact of the 2017 ACC/AHA high blood pressure guideline.* Circulation, 2018. **137**(2): p. 109-118.
22. Calhoun, D.A. and S.M. Harding, *Sleep and hypertension.* Chest, 2010. **138**(2): p. 434-443.
23. Ucak, S., et al., *Heart rate variability and obstructive sleep apnea: Current perspectives and novel technologies.* Journal of sleep research, 2021. **30**(4): p. e13274.
24. Milani, O.H., et al., *0537 Incident Hypertension Prediction in Obstructive Sleep Apnea using Machine Learning.* Sleep, 2023. **46**(Supplement_1): p. A236-A237.
25. Pun, C.K., et al., *On the design and implementation of FIR and IIR digital filters with variable frequency characteristics.* IEEE Transactions on Circuits and Systems II: Analog and Digital Signal Processing, 2002. **49**(11): p. 689-703.
26. Tan, M. and Q. Le. *Efficientnet: Rethinking model scaling for convolutional neural networks*. in *International conference on machine learning*. 2019. PMLR.
27. Zhang, X., et al. *Shufflenet: An extremely efficient convolutional neural network for mobile devices*. in *Proceedings of the IEEE conference on computer vision and pattern recognition*. 2018.
28. He, K., et al. *Deep residual learning for image recognition*. in *Proceedings of the IEEE conference on computer vision and pattern recognition*. 2016.
29. Deng, B., et al. *Cvxnet: Learnable convex decomposition*. in *Proceedings of the IEEE/CVF Conference on Computer Vision and Pattern Recognition*. 2020.

30. Li, Y., et al., *Efficientformer: Vision transformers at mobilenet speed.* Advances in Neural Information Processing Systems, 2022. **35**: p. 12934-12949.